

THE CORROSION BEHAVIOUR OF AUSTENITIC AND DUPLEX STAINLESS STEELS IN ARTIFICIAL BODY FLUIDS

KOROZIJSKO VEDENJE AVSTENITNEGA IN DUPEKSNEGA NERJAVNEGA JEKLA V SIMULIRANIH TELESNIH TEKOČINAH

Aleksandra Kocijan, Marjetka Conradi

Institute of metals and technology, Lepi pot 11, 1000 Ljubljana, Slovenia
aleksandra.kocijan@imt.si

Prejem rokopisa – received: 2009-09-29; sprejem za objavo – accepted for publication: 2009-11-11

The evolution of the passive film formed on duplex stainless steel 2205 and AISI 316L stainless steel in artificial saliva and a simulated physiological solution was studied using cyclic voltammetry and potentiodynamic measurements. The extent of the passive range slightly decreased with the increasing chloride concentration from artificial saliva to the simulated physiological solution. The formation of pits during the potentiostatic conditions was studied using atomic force microscopy and the results showed an increasing growth of pits for the AISI 316L compared to duplex stainless steel 2205 and, furthermore, a decreased corrosion resistance of both materials in the simulated physiological solution compared to the artificial saliva.

Keywords: duplex stainless steel, AISI 316L, potentiostatic, cyclic voltammetry, artificial saliva, simulated physiological solution

S ciklično voltametrij in z meritvami potenciodinamske polarizacije smo raziskovali tvorbo pasivne plasti na površini dupleksnega nerjavnega jekla 2205 in avstenitnega nerjavnega jekla AISI 316L v raztopini umetne slin in simulirani fiziološki raztopini. Z naraščajočo koncentracijo kloridnih ionov v simulirani fiziološki raztopini v primerjavi z umetno slino se je pasivno območje pri obeh materialih rahlo zožilo. Z uporabo mikroskopije na atomsko silo smo raziskovali pojav jamičaste korozije pod potenciostatskimi pogoji. Rezultati so potrdili povečano rast jamic pri AISI 316L v primerjavi z dupleksnim nerjavnim jeklom 2205 in bolj izrazito tvorbo le-teh z naraščajočo koncentracijo kloridnih ionov.

Ključne besede: dupleksno nerjavno jeklo, AISI 316L, potenciostatske meritve, ciklična voltametrij, umetna slina, fiziološka raztopina

1 INTRODUCTION

Austenitic stainless steel AISI 316L is the most commonly used orthopaedic and orthodontic bracket material. Its mechanical properties, such as ductility and wear resistance, make it attractive for particular applications. The corrosion resistance of stainless steel is relatively good. However, it is challenged by the hostile environment in the human body, as it is susceptible to localised corrosion in any environment containing chloride. Furthermore, it is well known that up to 22 % of the population may exhibit allergic and hypersensitivity reactions to nickel^{1,2}.

The 2205 duplex stainless steel is being investigated as a material for orthodontic bracket fabrication. The microstructure of this duplex stainless steel is a mixture of austenitic and delta-ferritic phases. The delta-ferrite is hard and relatively less ductile; the austenite is softer and more ductile. The combination of both phases results in a steel that is harder than the single-phase austenitic and more ductile than the single-phase ferritic stainless steel. The combination of both phases has a beneficial influence on the corrosion characteristics in various aqueous environments. The high Cr content together with high Mo and N contents gives rise to a high pitting-corrosion resistance in chloride solutions. The chromium adds to

the overall resistance through a passivation process by forming a complex spinel-type passive film (Fe, Ni)O(Fe, Cr)₂O₃. Molybdenum increases the stability of the passive film and, therefore, the ability of the stainless steel to resist the localised corrosion, including pitting and crevice corrosion, particularly in environments containing chloride ions³⁻⁸.

The evolution of the passive film formed on duplex stainless steel 2205 and AISI 316L stainless steel in artificial saliva and a simulated physiological solution was studied using cyclic voltammetry and potentiodynamic measurements. The formation of pits during the potentiostatic conditions was studied using atomic force microscopy (AFM, Nanoscope V, Veeco Instruments) in the contact mode.

2 EXPERIMENTAL

Duplex 2205 stainless steel and AISI 316 stainless steel were investigated. Their compositions were confirmed with analytical chemical methods, as shown in **Table 1**.

The experiments were carried out in artificial saliva (0.4 g/L NaCl, 0.4 g/L KCl, 0.795 g/L CaCl₂ × 2H₂O, 0.780 g/L NaH₂PO₄ × 9H₂O, 0.005 g/L Na₂S × 9H₂O,

Table 1: The composition of the 2205 duplex stainless steel and the AISI 316L (w/%)**Tabela 1:** Sestava dupleksnega nerjavnega jekla 2205 in AISI 316L (w/%)

	Cr	Ni	Mn	Si	P	S	C	Mo
2205	22.7	5.7	1.37	0.38	0.032	0.001	0.03	2.57
316L	17.0	10.0	1.40	0.38	0.041	< 0.005	0.021	2.10

1 g/L Urea) and in a simulated physiological solution – Hank's solution (8 g/L NaCl, 0.40 g/L KCl, 0.35 g/L NaHCO₃, 0.25 g/L NaH₂PO₄ × 2H₂O, 0.06 g/L Na₂HPO₄ × 2H₂O, 0.19 g/L CaCl₂ × 2H₂O, 0.41 g/L MgCl₂ × 6H₂O, 0.06 g/L MgSO₄ × 7H₂O, 1 g/L glucose). All the chemicals were from Merck, Darmstadt, Germany.

The test specimens were cut into discs of 15 mm diameter. The specimens were ground with SiC emery paper down to 1000 grit prior to the electrochemical studies, and then rinsed with distilled water. The specimens were then embedded in a Teflon PAR holder and employed as a working electrode. The reference electrode was a saturated calomel electrode (SCE, 0.242 V vs. SHE) and the counter electrode was a high-purity graphite rod. All the potentials described in the text are stated with respect to a SCE.

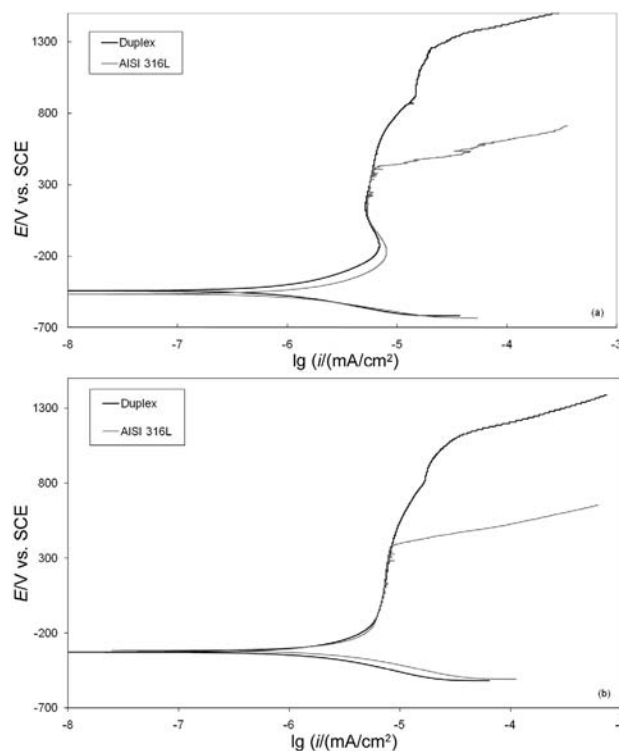
The cyclic voltammetry and potentiodynamic measurements were recorded using an EG&G PAR PC-controlled potentiostat/galvanostat Model 263 with M252 and Softcorr computer programs. In the case of potentiodynamic measurements the specimens were immersed in the solution 1 h prior to the measurement in order to stabilize the surface at the open-circuit potential. The potentiodynamic curves were recorded starting at 250 mV more negative than the open-circuit potential. The potential was then increased, using a scan rate of 1 mV s⁻¹, until the transpassive region was reached. In cyclic voltammetry a scan rate of 50 mV s⁻¹ was used, unless stated otherwise.

The passive layers on the surface of the 2205 DSS and AISI 316L were formed under potentiostatic conditions for 30 minutes at potentials of -0.6 V and 1.4 V vs. SCE, respectively. These potentials were selected in the region of transpassive oxidation of the polarization curve (see **Figure 1**). After the electrochemical preparation, the specimens were rinsed with distilled water and ethanol, dried and transferred to the analyzer chamber. To characterize the surfaces of the 2205 DSS and AISI 316L before and after exposing the samples to different corrosion conditions, such as artificial saliva and Hank's solution, AFM in the contact mode was used. The surface was probed with a commercial, sharpened, silicon nitride (Si₃N₄) cantilever, with a spring constant of 0.12 N/m. The topology of the surfaces was then analyzed with the Nanoscope V software.

3 RESULTS

Figure 1a shows the potentiodynamic curves for 2205 DSS and AISI 316L in artificial saliva and Hank's solution. After 1 h of stabilization at the open-circuit potential, the corrosion potential (E_{corr}) for the 2205 DSS in artificial saliva was approximately -0.44 V. Following the Tafel region, the alloy exhibited passive behaviour. However, the passive range is limited by the breakdown potential (E_b), which corresponds to the oxidation of water and the transpassive oxidation of the metal species. The breakdown potential for the 2205 DSS in artificial saliva was approximately 1.23 V. In the case of AISI 316L, the E_{corr} was approximately of -0.47 V and E_b was 0.37 V, respectively. The extent of the passive range slightly decreased with the increasing chloride concentration from artificial saliva to the simulated physiological solution. The corrosion potentials in Hank's solution were -0.32 V for 2205 DSS and AISI 316L (**Figure 1b**). The passive region was narrower compared to the results in artificial saliva due to the increased concentration of chloride ions. The breakdown potential shifted to more negative potentials for the 2205 DSS and AISI 316L in Hank's solution, i.e., 1.05 V and 0.35 V, respectively.

The cyclic voltammograms of the 2205 DSS and AISI 316L recorded in artificial saliva and Hank's solution make it possible to compare the current peaks

**Figure 1:** Polarisation curves recorded for the 2205 duplex stainless steel and the AISI 316L in (a) artificial saliva and (b) the simulated physiological solution**Slika 1:** Polarizacijske krivulje dupleksnega nerjavnega jekla 2205 in AISI 316L v (a) umetni slini in (b) simulirani fiziološki raztopini

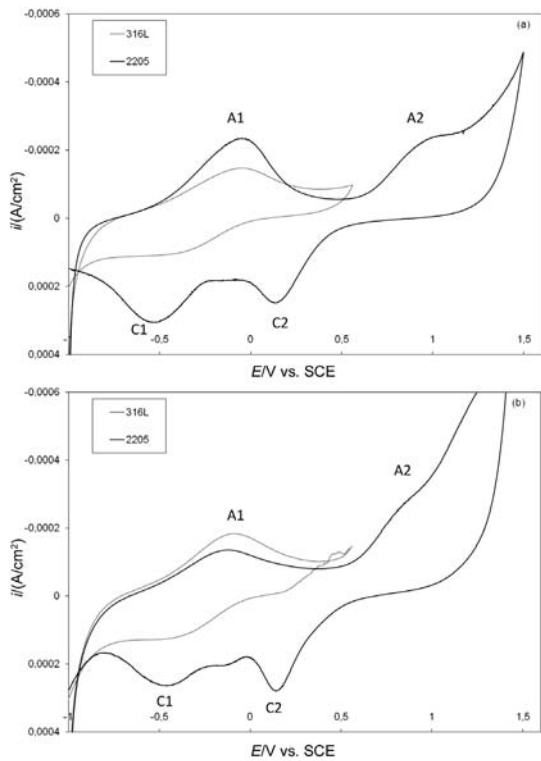


Figure 2: Cyclic voltammograms recorded for the 2205 duplex stainless steel and the AISI 316L in (a) artificial saliva and (b) the simulated physiological solution

Slika 2: Ciklični voltamogrami dupleksnega nerjavnega jekla 2205 in AISI 316L v (a) umetni slini in (b) simulirani fiziološki raztopini

and the corresponding electrochemical processes taking place on the materials investigated (**Figure 2**). The cyclic voltammograms were recorded for the AISI 316L and 2205 DSS at a scan rate of 50 mV/s, in the potential range from -1 V to 0.5 V and 1.5 V, respectively. As can be seen, the main characteristics of the cyclic voltammograms are similar in both solutions. In the presence of artificial saliva four peaks are observed in the cyclic voltammogram for the 2205 DSS (**Figure 2a**). The first anodic peak A1 at a potential -0.2 V can be ascribed to the electro-formation of Fe(II) hydroxide upon the Cr(III)-containing passivating layer, existing on the electrode at such negative potentials⁵. It is followed by the region with a constant current density, up to 0.9 V, where another peak A2 is observed in the transpassive region associated with the oxidation of Cr(III) to Cr(VI)⁹. The Ni(II) species formed during the passivation process might have been oxidised to Ni(IV) oxide (NiO_2) in this potential range, too. In the reduction cycle in the potential range of peak C2 at 0.2 V Cr(VI) is reduced to Cr(III) and the iron oxide-hydroxide layer is largely reduced in the potential range of peak C1 at a potential of -0.5 V⁹. In the case of AISI 316L in artificial saliva, only two peaks were observed in the cyclic voltammograms, the first one in the anodic cycle at -0.2 V, which can be ascribed to the electro-formation of Fe(II) hydroxide, and the second one in the cathodic cycle at -0.5 V, which corresponds to the reduction of the iron

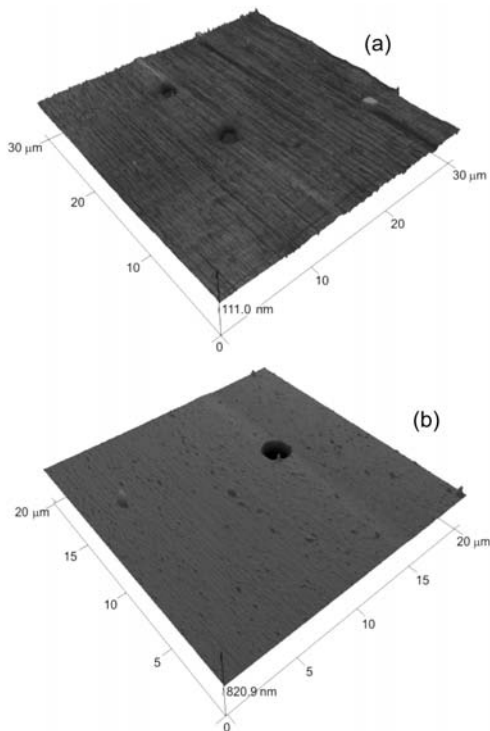


Figure 3: AFM images of the 2205 duplex stainless steel (a) and the AISI 316L (b) after oxidation in artificial saliva at 1.4 V and 0.65 V, respectively

Slika 3: AFM posnetek dupleksnega nerjavnega jekla 2205 (a) in AISI 316L (b) po oksidaciji v umetni slini pri $1,4$ V in $0,65$ V

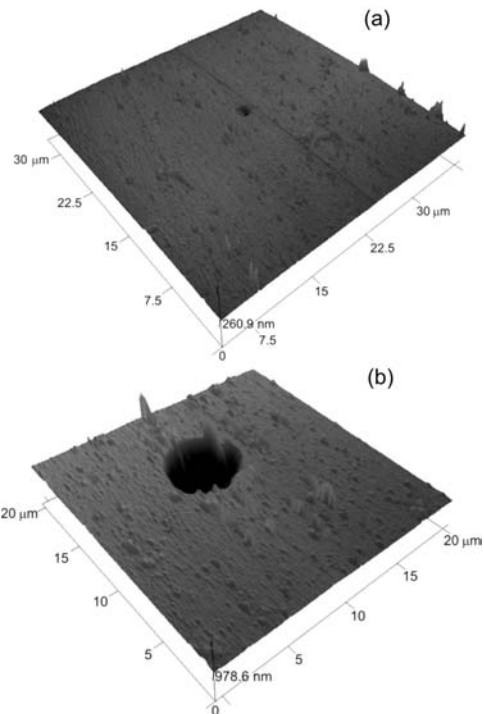


Figure 4: AFM images of the 2205 duplex stainless steel (a) and the AISI 316L (b) after oxidation in the simulated physiological solution at 1.4 V and 0.65 V, respectively

Slika 4: AFM posnetek dupleksnega nerjavnega jekla 2205 (a) in AISI 316L (b) po oksidaciji v simulirani fiziološki raztopini pri $1,4$ V in $0,65$ V

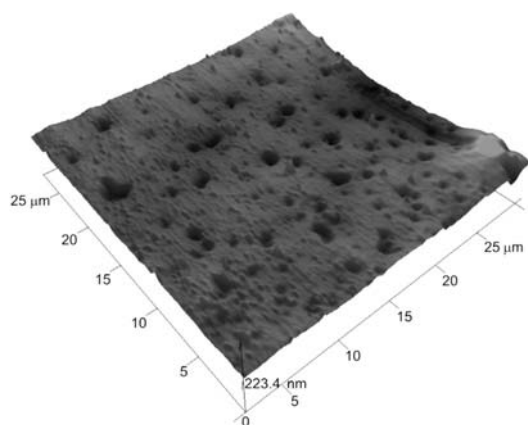


Figure 5: The surface of the AISI 316L treated with the simulated physiological solution. The formation of corrosion pits is significantly enhanced due to increased chloride concentration

Slika 5: Površina nerjavnega jekla AISI 316L v simulirani fiziološki raztopini. Tvorba korozivskih jamic je povečana zaradi vpliva višje koncentracije kloridnih ionov

oxide-hydroxide layer. In the presence of the simulated physiological solution the results were similar to the results obtained for artificial saliva (**Figure 2b**). However, due to the increased chloride concentration the corrosion current density enlarged compared to the artificial saliva. Similar results were obtained in different investigated media^{10–13}.

Figures 3 and 4 show AFM 3D height images of the 2205 DSS and AISI 316L surfaces when treated with artificial saliva and the simulated physiological solution, respectively. As a consequence of the corrosion, the formation of pits was observed on both surfaces. The degree of corrosion was reflected in the density of the pits that appeared on the surface, their shape and depth. Following this idea, the 2205 DSS sample indicated more resistance to corrosive solutions compared to the AISI 316L sample. The density of the pits on the 2205 DSS surface was small, the pits were shallow (few hundreds of nm) and not very well shaped, i.e., non-spherical. In contrast, on the surface of the AISI 316L sample an increased density of the pits was observed with depths up to a micrometer and more.

In addition, the simulated physiological solution appeared more aggressive than the artificial saliva for both samples due to the increased chloride solution. This effect was more pronounced for the AISI 316 L sample where the formation of corrosion pits was considerably enhanced over a larger area of the sample (**Figure 5**).

4 CONCLUSIONS

An electrochemical study of the passive film generated in artificial saliva and a simulated physiological solution on the DSS 2205 and AISI 316L was performed, and the results were analysed. Cyclic voltammograms obtained in the chloride solution showed characteristic peaks. The anodic peaks at -0.1 V and 0.9 V were identified with the formation of an iron oxide-hydroxide layer and the transpassive oxidation of Cr(III) to Cr(VI) and Ni(II) to Ni(IV), respectively. The reduction peaks at 0.2 V and -0.5 V are attributed to valence transitions, occurring in the solid state, associated with the chromium and iron in the oxide, respectively. None of the current peaks detected in the voltammetric curves can be attributed to the Mo species alone, which indicates that molybdenum mainly enhances the effect of other passivating species, i.e., Cr, more than acting directly in the passivating process in the chloride media.

The results of the electrochemical study showed an improved corrosion resistance of the 2205 DSS compared to the AISI 316L, which was also confirmed by the AFM imaging. Therefore, the present study indicates a possible exploitation of 2205 DSS in orthopaedic and orthodontic applications.

5 REFERENCES

- J. A. Platt, A. Guzman, A. Zuccari, D. W. Thornburg, B. F. Rhodes, Y. Ossida, D. W. Thornburg, B. F. Rhodes, Y. Ossida, B. K. Moore, *American Journal of Orthodontics and Dentofacial Orthopedics*, 112 (1997), 69–79
- R. D. Willenbruch, C. R. Clayton, M. Oversluisen, D. Kim, Y. Lu, *Corros. Sci.*, 31 (1990), 179–190
- R. M. Souto, I. C. Mirza Rosca, S. Gonzales, *Corrosion*, 57 (2001), 300–306
- F. Bernard, V. S. Rao, H. S. Kwon, *J. Electrochem. Soc.* 152 (2005) 10, 415–420
- F. J. Torres, W. Panyayong, W. Rogers, D. Velasquez-Plata, Y. Oshida, B. K. Moore, *Bio-Medical Mat. Eng.*, 8 (1998), 25–36
- A. Kocijan, Č. Donik, M. Jenko, *Corros. Sci.*, 49 (2007), 2083–2098
- K. T. Oh, Y. S. Kim, Y. S. Park, K. N. Kim, *J. Biomed. Mat. Res.*, 69B (2004), 183–194
- G. T. Burstein, C. Liu, *Corr. Sci.*, 49 (2007), 4296–4306
- N. Ramasubramanian, N. Preocanin, R. D. Davidson, *J. Electrochem. Soc.*, 132 (1985), 793–798
- Č. Donik, A. Kocijan, M. Jenko, A. Drenik, B. Pihlar, *Corros. Sci.* 51 (2009) 827–832
- A. Kocijan, Č. Donik, M. Jenko, *Mater. tehnol.*, 43 (2009), 39–42
- Č. Donik, A. Kocijan, M. Jenko, I. Paulin, *Mater. tehnol.*, 43 (2009), 137–142
- A. Kocijan, Č. Donik, M. Jenko, *Mater. tehnol.*, 43 (2009), 195–199